ResearchGate

See discussions, stats, and author profiles for this publication at: https://www.researchgate.net/publication/5274308

Molecular Dynamics Study of the Solvation of an α-Helical Transmembrane Peptide by DMSO

ARTICLE *in* THE JOURNAL OF PHYSICAL CHEMISTRY B · AUGUST 2008

Impact Factor: 3.3 · DOI: 10.1021/jp076678j · Source: PubMed

CITATIONS
16

READS
21

3 AUTHORS, INCLUDING:

Afonso Duarte
New University of Lisbon
24 PUBLICATIONS **252** CITATIONS

SEE PROFILE

Available from: Afonso Duarte
Retrieved on: 26 January 2016

Molecular Dynamics Study of the Solvation of an α-Helical Transmembrane Peptide by DMSO

Afonso M. S. Duarte,[†] Carlo P. M. van Mierlo,[‡] and Marcus A. Hemminga*,[†]

Laboratory of Biophysics and Laboratory of Biochemistry, Wageningen University, Dreijenlaan 3, 6703 HA Wageningen, The Netherlands

Received: August 20, 2007; Revised Manuscript Received: February 6, 2008

A 10-ns molecular dynamics study of the solvation of a hydrophobic transmembrane helical peptide in dimethyl sulfoxide (DMSO) is presented. The objective is to analyze how this aprotic polar solvent is able to solvate three groups of amino acid residues (i.e., polar, apolar, and charged) that are located in a stable helical region of a transmembrane peptide. The 25-residue peptide (sMTM7) used mimics the cytoplasmic proton hemichannel domain of the seventh transmembrane segment (TM7) from subunit *a* of H^+-V-ATPase from *Saccharomyces cerevisiae*. The three-dimensional structure of peptide sMTM7 in DMSO has been previously solved by NMR spectroscopy. The radial and spatial distributions of the DMSO molecules surrounding the peptide as well as the number of hydrogen bonds between DMSO and the side chains of the amino acid residues involved are extracted from the molecular dynamics simulations. Analysis of the molecular dynamics trajectories shows that the amino acid side chains are fully embedded in DMSO. Polar and positively charged amino acid side chains have dipole−dipole interactions with the oxygen atom of DMSO and form hydrogen bonds. Apolar residues become solvated by DMSO through the formation of a hydrophobic pocket in which the methyl groups of DMSO are pointing toward the hydrophobic side chains of the residues involved. The dual solvation properties of DMSO cause it to be a good membrane-mimicking solvent for transmembrane peptides that do not unfold due to the presence of DMSO.

Introduction

The study of the conformational properties of transmembrane proteins and peptides is an expanding and challenging area in biophysics. One of the major challenges in the field is the selection of a suitable solvent that solubilizes the transmembrane proteins and peptides under investigation while still mimicking relevant properties of a biomembrane. For example, high-resolution liquid-state NMR spectroscopy becomes then an excellent technique to obtain information at the atomic level about the conformational properties of peptides in a membrane-mimicking solvent.

A membrane-mimicking solvent needs to reproduce as best as possible the transmembrane environment of the transmembrane protein or peptide under investigation. In this study, we focus on the solubilization of a transmembrane peptide that is a segment of the large transmembrane protein V-ATPase from *Saccharomyces cerevisiae*. In the case of a transmembrane peptide in its native environment, two extreme situations can occur: (i) the peptide is fully embedded in the lipid bilayer and the solvent should thus mimic hydrophobic lipid acyl chains, or (ii) the peptide is surrounded by other transmembrane protein segments and the solvent should then mimic protein−protein interactions. A mixture of both situations can also occur. In the first situation, the corresponding membrane-mimicking solvent should solubilize hydrophobic amino acid side chains and should have a low polarity and low dielectric constant. In the second situation, a solvent is required that is able to solvate hydrophobic, hydrophilic, and charged amino acid residues.

Membrane-mimicking organic solvents are not able to provide the specific amphipathic environments found in biomembranes. However, organic solvents can mimic to a certain level the hydrophobic character of a biomembrane and some organic solvents mimic the hydrophilic character of the membrane interface. In the case of transmembrane peptides two organic solvents have been identified to be relatively good mimics of membranes: TFE (2,2,2-trifluoroethanol) and DMSO (dimethyl sulfoxide, $(CH_3)_2S{=}O$).

TFE has been used during the past decades to solubilize peptides, and it stabilizes either α-helix or *β*-sheet conformers.[1] This property has been attributed to its small relative dielectric constant ($\varepsilon = 26.7$;[2] dipole moment = 2.52 D[2]) and because it does not disrupt hydrogen bonds between backbone amide and carbonyl groups. In addition, TFE interacts only weakly with apolar amino acid residues and thus does not disrupt inter-residue van der Waals interactions, thereby conserving the tertiary structure of proteins.[1,3]

Several studies have demonstrated that the organic solvent DMSO can be used as an alternative for TFE, detergent micelles, and lipid bilayers, for example to study the behavior of α-helical transmembrane peptides in a membrane-mimicking solvent.[4–9] An advantage of DMSO over other organic solvents arises from its aprotic physical properties (small relative dielectric constant ($\varepsilon = 46.8$[2]) and high dipole moment (4.0 D[2])), which are the origin of its good ability to solubilize hydrophobic helical peptides. On the other hand, it is known that the use of DMSO in aqueous protein solutions above a certain concentration can lead to peptide unfolding or protein denaturation, due to a disruption of the intramolecular backbone hydrogen bonds.[10,11]

* To whom correspondence should be addressed. Telephone: +31317482635. Fax: +31-317-482725. E-mail: marcus.hemminga@wur.nl. Web site: http://ntmf.mf.wau.nl/hemminga.

[†] Laboratory of Biophysics.

[‡] Laboratory of Biochemistry.

10.1021/jp076678j CCC: $40.75 © 2008 American Chemical Society
Published on Web 06/27/2008

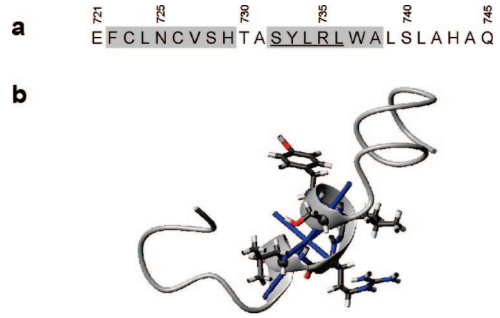

Figure 1. Conformational properties of peptide sMTM7 in DMSO. (a) Primary structure of peptide sMTM7. The gray boxes represent the helical regions identified in DMSO.[8] The five residues of which the MD simulations in DMSO are analyzed are underlined. The numbering of the residues is according to the numbering of the entire subunit *a* from V-ATPase.[34] (b) Ribbon representation of the lowest-energy NMR-derived three-dimensional structure of peptide sMTM7 in DMSO (PDB ID 2NVJ).[8] The α-helix axis and corresponding perpendicular axis of the second helical section of peptide sMTM7 are depicted in blue. The residues under study are shown in stick representation (blue, nitrogen; red, oxygen; black, carbon; white, hydrogen). The conformations are drawn with MOLMOL.[35]

To gain insight in the DMSO-solvating properties of transmembrane peptides, we present in this paper a molecular dynamics (MD) simulation study of a transmembrane peptide (peptide sMTM7, Figure 1a). In the literature MD simulations have been reported on studies of the secondary structure and folding properties of peptides in DMSO.[12–15] Peptide sMTM7 represents the naturally occurring sequence of the seventh transmembrane segment (TM7) of the H^+-V-ATPase pump from *Saccharomyces cerevisiae*. The peptide is located in subunit *a* and is known to be involved in the cytoplasmic proton translocation mechanism in the enzyme via the interaction of different amino acid residues[16,17] with neighboring transmembrane helical segments. This interface is proposed to be part of the proton translocation channel. Three amino acid residues were identified in its primary structure that actively participate in the cytoplasmic proton translocation hemichannel (i.e., H729, R735, and H743).[8,16] In the MD simulations peptide sMTM7 is assumed to be solubilized in DMSO. Peptide sMTM7 was designed previously for the purpose of structural studies using circular dichroism (CD), ESR, and NMR spectroscopies.[8,18] Peptide sMTM7 is composed of 25 amino acid residues, and throughout this article their numbering is based on the sequence of the full-length subunit *a* from V-ATPase (Figure 1a). The conformation of the TM7 domain has been studied by several spectroscopic techniques in the following environments: lipid bilayers (by fluorescence resonance energy transfer (FRET) and CD),[19] SDS micelles (by ESR and CD),[7,20] and DMSO (by high-resolution NMR).[7,8] In all these environments the TM7 domain is mainly α-helical.

An atomistic structure of peptide sMTM7 in d_6-DMSO was obtained from high-resolution liquid-state NMR spectroscopy (PDB ID 2NVJ).[8] It reveals two helical sections that are separated by a flexible hinge of two amino acid residues, i.e., T730 and A731 (Figure 1b). The 20 lowest-energy conformations[8] show that the side chains of the amino acid residues S732 to A738 of the second α-helical section of peptide sMTM7 do not have contacts with one another. Furthermore, in the lowest-energy conformer the amino acid side chains are oriented perpendicular to the helical axis (Figure 1b). This observation implies that the side chains are fully embedded in DMSO. Indeed, the $N_{\eta 1}$, $N_{\eta 2}$, and N_{ε} guanidinium protons of R735, the side chain of which is positively charged, give rise to three chemical shift values. Both $N_{\eta 1}$ protons of R735 give rise to one chemical shift position, because they do not participate in interresidue hydrogen bonds and are fully accessible to DMSO. A similar observation was made for the $N_{\eta 2}$ protons. The NMR studies of sMTM7 showed the presence of a disulfide bridge between C723 and C726,[8] and in that same study residue R735 was considered to be positively charged. Thus for all MD simulations performed in this study a disulfide bridge between C723 and C726 was included and the R735 was taken to be charged. Also the peptide termini were considered to be charged.

TABLE 1: Starting Conformations of Peptide sMTM7 Used during the MD Simulations and Number of DMSO Molecules Involved[a]

simulation no.	starting conformation	no. of DMSO molecules
1	lowest-energy NMR-derived three-dimensional structure	4371
2	α-helix	4444
3	extended	4201

[a] All simulations were carried out at 300 K and run for a period of 10 ns.

In this paper we present a MD study on the solvation of peptide sMTM7 by DMSO. The duration of the simulations was on the order of nanoseconds, which allows us to have a representation of the dynamics of the solvent. However, we should point out that, due to the time frame used in the MD calculations, no analysis of the changes in the secondary structure of the peptide could be made. To analyze the solvation of the peptide, the radial and spatial distributions of DMSO molecules around the peptide were calculated. In particular, analysis of the interactions of DMSO with the side chains of the residues in the helical regions of peptide sMTM7 is useful as these side chains are fully embedded in DMSO. The questions addressed are the following: (i) What is the nature of the interactions between the peptide and DMSO? (ii) Do these interactions resemble the ones the peptide experiences in its native environment? To answer these questions, an analysis is made of the MD trajectories of three groups of amino acid residues (i.e., apolar, polar, and charged) within the second helical region of peptide sMTM7.

Computational Methods

Molecular Dynamics Simulations of sMTM7 in DMSO. To study the solvation properties of DMSO, the MD trajectories of DMSO surrounding apolar residues L734 and L736, polar residues S732 and Y733, and charged residue R735 of peptide sMTM7 were analyzed.

The MD simulations of peptide sMTM7 were carried out in pure DMSO. Three starting conformations were used: the published lowest-energy NMR-derived three-dimensional structure[8] (MD simulation no. 1 in Table 1), the peptide being fully α-helical (MD simulation no. 2 in Table 1), and the peptide being in an extended conformation (MD simulation no. 3 in Table 1). For all simulations the C- and N-termini of peptide sMTM7 were charged. The MD simulation that started with the peptide in an extended conformation enables the evaluation of the effects of potential hydrogen bond formation between the peptide backbone and DMSO. During the three MD simulations the guanidine group of R735 was in the protonated guanidinium form. Both starting conformations of the fully α-helical and extended conformations of peptide sMTM7 were generated by taking into account the conventional backbone torsion angles using the PyMOL software.[21]In the case of the

fully α-helical conformation the angle between the side chains and the helical axis was set to 90°.

The MD simulations were performed with GROMACS 3.3.1,[22,23] using the GROMOS96 43A1[24] force field. The simulations were run for a period of 10 ns at 300 K in explicit DMSO using the model of Liu.[25] Analysis of the trajectories was performed using the programs included in the GROMACS package.

The peptide was placed in a cubic box of explicit DMSO with a minimum distance solute box of 20 Å. The number of DMSO molecules used during each MD simulation is given in Table 1. The volume of the molecular dynamics box used for the different simulations was, for simulation no. 1, 492.8 nm^3; for simulation no. 2, 503.4 nm^3; and for simulation no. 3, 463.3 nm^3. Periodic boundary conditions were applied. Each system was first energy-minimized in 2000 steps by using the steepest-descent algorithm. Each system was equilibrated in a 5 ns position-restrained simulation, during which the force constant of the position restraints term for the solute was decreased from 1000 to 0 $kJ \cdot mol^{-1} \cdot nm^{-2}$. The initial velocities were generated at 300 K following a Maxwellian distribution. The simulations were performed at constant pressure (100 kPa) and temperature (300 K) by weakly coupling the system to external temperature[26] and pressure baths, except for the first 20 ps equilibration part that was performed at constant volume. All bonds were constrained by using the LINCS algorithm.[27] The peptide and the solvent were coupled separately to a temperature bath with a time constant of 0.1 ps. The pressure was coupled to an external bath at 100 kPa with a time constant of 0.5 ps and a compressibility of 4.5×10^{-3} kPa^{-1}. A twin-range cutoff of 0.8 and 1.4 nm was used for the nonbonded interactions. A 2-fs time step was used for the leapfrog algorithm integration. The simulations were performed on a Linux workstation with two dual-core processors (Intel Xeon 3.06 GHz), or on a Sun cluster under Linux having eight dual-core processors (Intel Xeon 2.80 GHz) using the parallel version of GROMACS.

Analysis of Molecular Dynamics Trajectories. The time-dependent development of the secondary structure of the peptide was determined from the full 10-ns MD trajectories by GROMACS using the DSSP protocol.[28]

The solvation of peptide sMTM7 by DMSO was studied by calculating the radial distribution function (rdf) of the oxygen (i.e., $g_{X-O}(r)$) and the methyl groups (i.e., $g_{X-Me}(r)$) of DMSO around atom X of peptide sMTM7 under investigation, using the following equation:

$$g_{A-B}(r) = \frac{\rho_B(r)}{(\rho_B)_{total}} \quad (1)$$

with $\rho_B(r)$ representing the density of atom B around atom A at an interatomic distance r, and $(\rho_B)_{total}$ the particle density of atom B averaged over an sphere with 10 Å radius around the center of atom A.[29,30] Both methyl groups of DMSO were treated as one average group during the calculations because we obtained the same radial distribution values using two separate methyl groups per DMSO molecule (data not shown). Of the amino acid residues investigated the following atoms or group of atoms were studied: the oxygen atom of the hydroxyl group of S732 and Y733, the nitrogen atoms of the guanidine group of R735, and the methyl groups of L734 and L736 (the hydrogen and carbon atoms that comprise an individual methyl group were treated as a pseudogroup). As opposed to the radial distribution function, the spatial distribution function (sdf) gives the density of DMSO in Cartesian space. Both rdf and sdf functions were calculated using the full 10-ns MD trajectories.

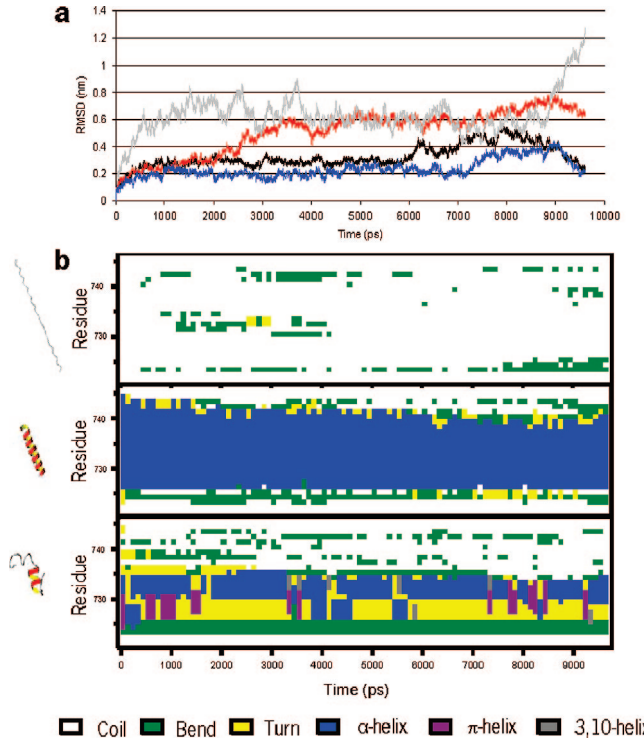

Figure 2. Analysis of MD simulations of peptide sMTM7 in DMSO. (a) rmsd values obtained during the MD simulations of the backbone of peptide sMTM7. Three starting conformations are used: the lowest-energy NMR-derived three-dimensional structure (MD simulation no. 1) (red), the peptide being fully α-helical (MD simulation no. 2) (black), and the peptide being an extended conformation (MD simulation no. 3) (gray). The rmsd values of the backbone atoms of residues S732-L736 (the second helical region of sMTM7) during MD simulation no. 1 are shown in blue. (b) Time-dependent behavior of the secondary structure of peptide sMTM7 calculated using DSSP:[28] bottom, lowest-energy NMR-derived three-dimensional structure (MD simulation no. 1); middle, fully α-helical starting conformation (MD simulation no. 2); and top, extended conformation (MD simulation no. 3). The plots are calculated using the full 10-ns MD trajectory and a 1000-fs time frame.

The hydrogen bonds formed by peptide sMTM7 and by DMSO were identified using a geometric criterion of a minimum distance between donor and acceptor of 0.35 nm and a maximum of 30° for the angle between the donor hydrogen and the distance between acceptor and donor.[30]

Results and Discussion

Time-Dependent Behavior of the Secondary Structure of sMTM7. The spatial and radial distribution functions of DMSO molecules solvating other DMSO molecules were determined for all MD simulations in this study (data not shown). The results obtained are comparable to the published data.[31] In this paper we employ MD simulations to obtain detailed information on the solvation of peptide sMTM7 by DMSO molecules. The MD simulations show that the three sMTM7−DMSO systems (Table 1) are equilibrated, because the fluctuations in temperature, pressure, density, and total energy (potential + kinetic) of the system are minimal. During the final 5 ps of the MD simulations the average temperature is 300.0 ± 4 K, the pressure 1.6 bar, and the density 1139 kg/m^3 with fluctuations less than 1%. The fluctuations in total energy are less than 0.2%.

In Figure 2 the backbone rmsd (root-mean-square deviation) values and secondary structure analysis of the three MD simulations are depicted. In the case of MD simulation no. 1

(which starts with the lowest-energy NMR-derived three-dimensional structure), the rmsd values of the backbone slightly increase up to 3.5 ns and then fluctuate around 0.6 nm (Figure 2a). After 8 ns an increased fraying is observed in the C-terminus (see Figure 2b). Within 1 ns the rmsd values of the fully helical sMTM7 starting conformation (MD simulation no. 2) stabilize, and after 6.5 ns a slight increase in rmsd values is observed due to some fraying of the C-terminus (Figure 2b). Since we focus on the interactions of DMSO with the amino acid residues in the region S732-L736 of peptide sMTM7, the rmsd values of this region of the peptide during MD simulation no. 1 are plotted as well (Figure 2a). As this region is helical (Figure 2b), the corresponding rmsd values are similar to the ones found for MD simulation no. 2 (which starts with fully α-helical sMTM7). The rmsd values observed after 2.5 ns in simulation no. 1, which starts with the lowest-energy NMR-derived three-dimensional structure, are higher than those observed during the MD simulations of the fully helical starting conformation and of the region S732-L736 of the lowest-energy NMR-derived three-dimensional structure. These high rmsd values of peptide sMTM7 are caused by the fraying of the C-terminus, the presence of a flexible hinge at T730, and the dynamic first helical section, which adopts turn, bend, and π-helical conformations. These features have been previously identified by NMR spectroscopy.[8] Starting with peptide sMTM7 in an extended conformation (MD simulation no. 3), a stable rmsd value of 0.6 nm is reached within 1 ns and lasts for another period of 8 ns.

The time-dependent behavior of the secondary structure of peptide sMTM7 is shown in Figure 2b. Occasionally bend, coil, and turn conformations are observed during the time trajectory of the MD simulation that starts with peptide sMTM7 as a full α-helix (MD simulation no. 2). A much lower helical content is observed during the MD simulations of the lowest-energy NMR-derived three-dimensional structure of peptide sMTM7 (MD simulation no. 1). However, the α-helical region under investigation (S732-L736) is relatively stable during the simulation period. As a consequence, the DMSO solvent shell around the side chains of residues S732-L736 should be not much affected during the MD simulation period by conformational changes of the backbone of the peptide.

Hydrogen Bonds between sMTM7 and DMSO. To analyze whether the backbone hydrogen bonds of peptide sMTM7 are disrupted by DMSO during the MD simulation period, the number of NH···O=S$(CH_3)_2$ bonds is tracked as a function of time during all three MD simulations (Figure 3). The fluctuations observed in the number of hydrogen bonds between DMSO and sMTM7 during the MD simulations show that the peptide undergoes small conformational changes as a function of time.

In the case of MD simulation no. 3 (extended conformation), one expects that all 25 backbone amide hydrogen atoms are exposed to DMSO. Indeed, many NH···O=S$(CH_3)_2$ hydrogen bonds (on average about 20) are observed, indicating that almost no hydrogen bonds between backbone amides and carbonyls are present during the MD simulation period. In the cases of MD simulation no. 1 (lowest-energy NMR-derived three-dimensional starting conformation) and MD simulation no. 2 (fully α-helical starting conformation), the average number of NH···O=S$(CH_3)_2$ bonds observed during the MD simulation period is much lower (i.e., 12 and 7 NH···O=S$(CH_3)_2$ bonds, respectively) (Figure 3).

During all three MD simulations the number of hydrogen bonds becomes constant within a few nanoseconds. The backbone of S732-L736 of peptide sMTM7 virtually has no

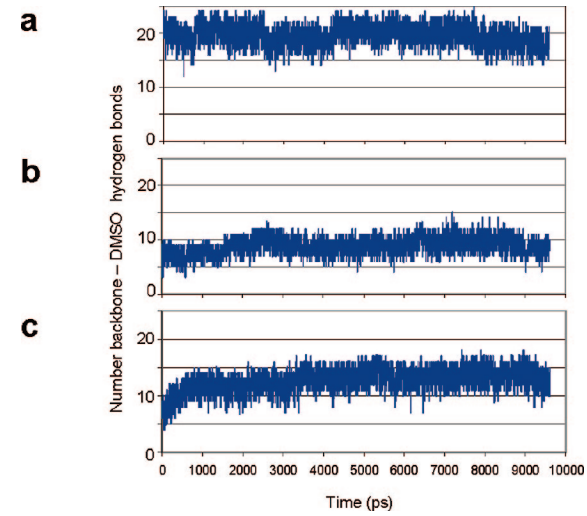

Figure 3. Number of hydrogen bonds that are formed between the backbone of peptide sMTM7 and DMSO (NH···O=S$(CH_3)_2$) during the MD simulation period. (a) Extended starting conformation of peptide sMTM7 (MD simulation no. 3), (b) fully α-helical starting conformation of peptide sMTM7 (MD simulation no. 2), and (c) lowest-energy NMR-derived three-dimensional structure of peptide sMTM7 (MD simulation no. 1). The plots are calculated using the full 10-ns MD trajectory and a 100-fs time frame.

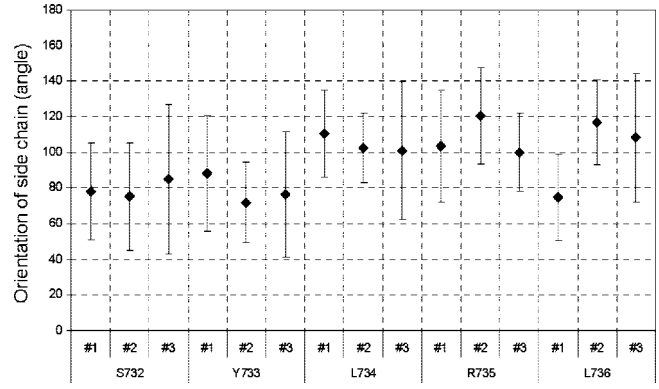

Figure 4. Orientation of the side chains of the amino acid residues in the S732-L736 segment of peptide sMTM7. The orientation is defined as the angle that is formed between the long axis of segment S732-L736 and the vector that links C_β with the outermost heavy atom of the particular side chain involved. The angles (◆) are calculated from the full 10-ns trajectory of each individual MD simulation: no. 1 (lowest-energy NMR-derived three-dimensional structure), no. 2 (fully α-helical conformation), and no. 3 (extended conformation). Angles are shown together with the corresponding standard deviations.

hydrogen bond with DMSO when starting the MD simulation with peptide sMTM7 in a fully α-helical conformation (MD simulation no. 2) (data not shown). The same region has only one intermolecular hydrogen bond with DMSO in a small number of time frames when starting the MD simulation with the lowest-energy NMR-derived three-dimensional structure (MD simulation no. 1). Thus, on the time scale of the MD simulations, DMSO does not disrupt the hydrogen bonds between the backbone atoms of S732-L736 of peptide sMTM7.

Orientation of the Amino Acid Side Chains of the S732-L736 Segment. No side chain interactions between neighboring residues are observed for residues S732-L736 of peptide sMTM7 in all three MD simulations done. The absence of such interactions is highlighted in Figure 4, which shows the orientation of the corresponding side chains. The side chain orientation is defined as the angle that is formed between the long axis of segment S732-L736 and the vector that links C_β

TABLE 2: Radial Distribution Function Maxima (in nm) Obtained for the Solvation Shells of DMSO Around Specific Atoms or Group of Atoms of the S732-L736 Segment of Peptide sMTM7[a]

	S732	Y733	L734	R735		L736
	X = OH	**X = OH**	**X = Me**	**X = $N_{\eta 1}$, $N_{\eta 2}$**	**X = N_{ε}**	**X = Me**
$g_{X-O}(r)$	0.25	0.25	0.7	0.3	0.4	0.7
	0.55	0.55		0.5	0.3	
					0.5	
$g_{X-Me}(r)$	0.35	0.35	0.4	0.39	0.56	0.4
			0.6	0.56		0.6

[a] The atom or group of atoms X studied are marked in bold. The MD simulation results obtained with the lowest-energy NMR-derived three-dimensional structure have been used to calculate the radial distribution functions of the oxygen and methyl groups of DMSO.

and the outermost heavy atom of the side chain involved.[32] Although the various side chains exhibit different dynamics, their orientation is on average perpendicular to the long axis of the segment. The side chains mentioned do not interact with one another but mainly interact with DMSO. As the amino acid side chains are fully embedded in DMSO during the whole 10-ns MD trajectory and no intraresidual interactions are observed, the entire MD trajectory can be used to analyze how DMSO solvates the side chains of the residues under investigation. Thus, information about the solvation shells surrounding particular amino acid residues can be extracted.

Determination of Solvation Shells of DMSO Around Amino Acid Side Chains of the S732-L736 Segment. The solvation of amino acid residues S732-L736 of peptide sMTM7 in DMSO is studied by calculating the radial distribution function (rdf) of the oxygen (i.e., $g_{X-O}(r)$) and of the methyl (i.e., $g_{X-Me}(r)$) of DMSO around various selected atoms and groups of atoms (X) of these residues. Thus, information about the local concentration and orientation of DMSO molecules around an amino acid residue of interest is obtained and this enables the visualization of the corresponding solvent shell. Solvation shells calculated for the MD simulations of the lowest-energy NMR-derived three-dimensional structure (MD simulation no. 1) of residues S732-L736 of peptide sMTM7 in DMSO are listed in Table 2 and are schematically shown in Figure 5. Similar results are obtained when starting the MD simulation with peptide sMTM7 in different starting configurations, such as a full α-helix, or an alternative extended structure (results not shown). The solvation shells are discussed in detail in the following sections.

Radial distribution function calculations of MD simulations no. 1 and no. 2 (i.e., starting with the lowest-energy NMR-derived three-dimensional structure and fully helical conformation, respectively) show that no shell of oxygen atoms of DMSO is found in the vicinity of the backbone amide hydrogens of the second helical region of the peptide. Indeed, during the 10-ns MD simulations the helical conformation of the region S732-L736 of peptide sMTM7 is not disrupted by the presence of DMSO. In contrast, the MD simulations of peptide sMTM7 in an extended starting conformation (MD simulation no. 3) show that a shell of oxygen atoms of DMSO is found around the amide hydrogens of peptide sMTM7 (data not shown). In this shell, the distance between an individual oxygen atom of DMSO and amide hydrogen is 0.2−0.3 nm. This distance is consistent with the formation of a hydrogen bond between DMSO and the amide hydrogens involved.

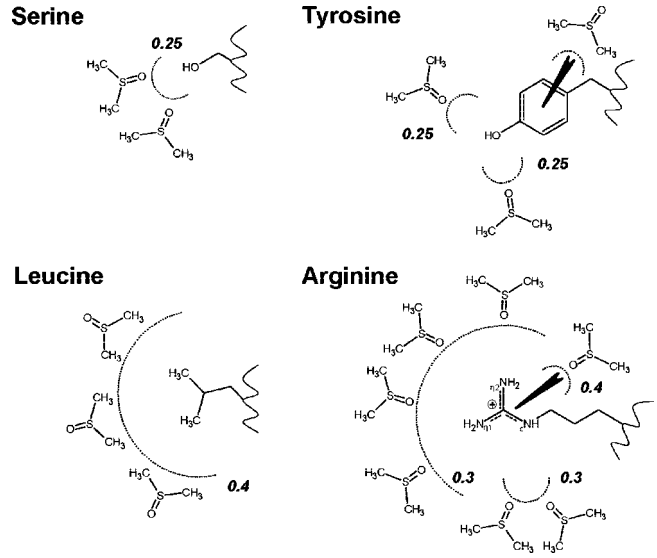

Figure 5. Schematic illustration of the layer of DMSO molecules that surrounds the side chains of residues S732-L736 of peptide sMTM7. The solvent layers are determined based on the radial and spatial distribution function results. Shown is the first solvation shell that surrounds the OH groups of S732 and Y733, the methyl groups of leucines L734 and L736, and the side chain nitrogen atoms of R735, respectively (as indicated by a dotted line). The radial distribution function maxima are given in nanometers. The number of DMSO molecules used to represent a shell is merely illustrative and not quantitatively correct.

Solvation of the Side Chains of S732 and Y733 of sMTM7 by DMSO. The radial distribution functions $g_{O-O}(r)$ of the oxygen of DMSO around the OH of both S732 and Y733 are very similar and show maxima at 0.25 and 0.55 nm (Figure 6 and Table 2). However, the corresponding spatial distribution functions of DMSO differ significantly. In the case of serine, the oxygen atoms of DMSO form a "spherical-like cloud" close to the proton of the OH group (Figure 6a), whereas in the case of tyrosine they form a "ring-like cloud" in the vicinity of the proton of the OH group (Figure 6b). The radial distribution function $g_{O-Me}(r)$ of the methyls of DMSO around the OH of both S732 and Y733 show that they form a shell at 0.35 nm around this group (Table 2, Figure 6). Thus, two $g_{O-O}(r)$ shells are intercalated by a $g_{O-Me}(r)$ shell and the DMSO molecules involved have a specific orientation with respect to the OH groups of S732 and Y733, respectively. The oxygen atoms of the solvent DMSO are oriented toward the hydrogen atom of the hydroxyl group involved (Figures 5 and 6).

The differences observed between the spatial distributions of the oxygen of DMSO around the OH groups of S732 and Y733 are due to the differing orientations the corresponding O−H bonds can sample. In the case of tyrosine, the aromatic ring causes the O−H bond to occupy a space that is described by a cone. As a consequence, the oxygen of DMSO molecules is spatially distributed as a ring at the base of this cone (Figure 6b). In the case of the hydroxyl group of serine, no such sterical restriction applies and therefore the spatial distribution of the oxygen atom of DMSO is a "spherical cloud" close to the proton of its OH group (Figure 6a).

The observation that both $g_{O-O}(r)$ functions discussed have a maximum at 0.25 nm suggests the presence of a strong hydrogen bond between DMSO and the hydrogen atom of the OH groups of S732 and of Y733, respectively. During the full 10-ns MD trajectory only one such stable hydrogen bond is observed for both residues. Compared to the other amino acid

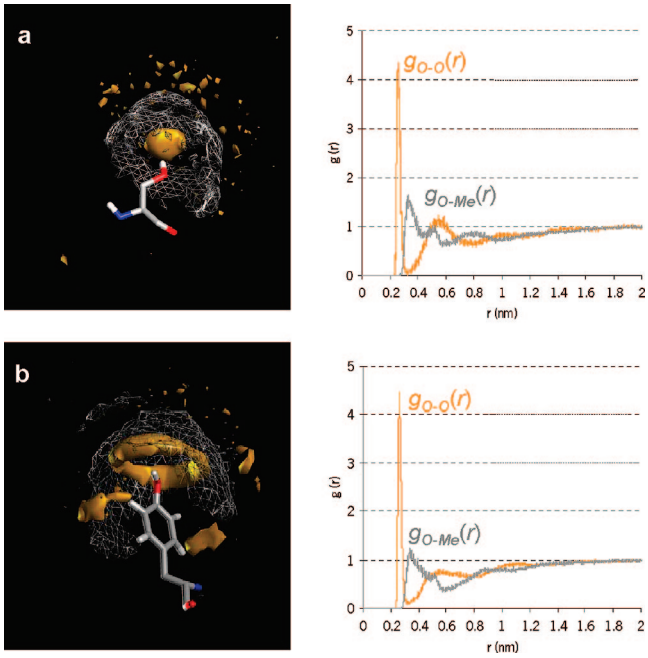

Figure 6. Radial distribution functions (right) of the oxygen and methyl groups of DMSO around the OH groups of S732 (a) and Y733 (b). The corresponding spatial distribution functions are shown on the left-hand side of the figure. The oxygen atom of DMSO is depicted as an orange surface, and the methyl group is depicted as a gray mesh. The amino acid residues are shown in stick representation. The plots are calculated using the full 10-ns MD trajectory that starts with the lowest-energy NMR-derived three-dimensional structure of peptide sMTM7 embedded in DMSO (simulation no. 1).

residues investigated, these hydrogen bonds are the strongest observed in this study. The maximum at 0.25 nm is consistent with the typical average distance between the hydrogen bond donor and acceptor of hydroxyl−hydroxyl (OH···OH) or hydroxyl−carbonyl (OH···O═C) groups, which is 0.28 nm (±0.3 nm).[33]

The second shell of DMSO molecules that surrounds the OH groups of S732 and Y733 has a maximum in its radial distribution function $g_{O-O}(r)$ at 0.55 nm (Figure 6, Table 2). This second layer of ordered DMSO molecules arises due to the presence of an ordered first layer of DMSO molecules that surrounds the OH group of the amino acids involved. As the second layer of DMSO molecules is not involved in direct hydrogen bonding with the OH groups mentioned, these DMSO molecules are much less ordered than the ones in the first layer. The value of the radial distribution function $g_{O-O}(r)$ at 0.55 nm of S732 is higher than the corresponding value calculated for Y733. Moreover, a major difference in the distribution of the oxygen atoms of DMSO in the second solvation shell is identified by determining the spatial distribution function (Figure 6). In the case of S732, the second $g_{O-O}(r)$ shell is located outside the first $g_{O-Me}(r)$ shell and this shell is not ordered much. However, in the case of tyrosine another shell of oxygen atoms of DMSO is observed coplanar to the face of the aromatic ring. This shell has a maximum radial distribution function value positioned at 0.57 nm from the center of the aromatic ring (data not shown). This $g_{O-O}(r)$ shell of DMSO molecules that surrounds the aromatic ring of tyrosine is well organized, and the corresponding DMSO molecules direct their methyl groups toward the aromatic ring. In the case of serine, the second DMSO shell is already part of the bulk solvent. In addition, an extra shell of methyl groups of DMSO is observed that faces

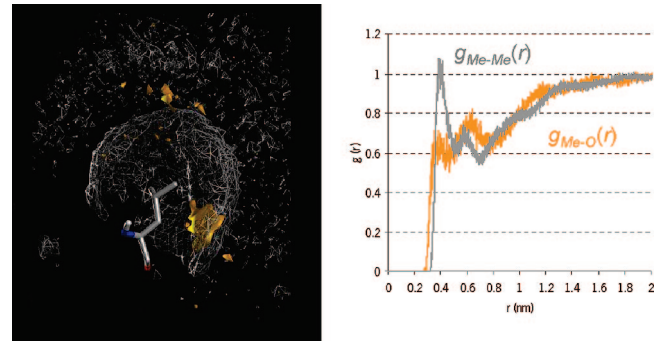

Figure 7. Radial distribution function (right) of the oxygen and methyl groups of DMSO around the methyl groups of L734 and L736, respectively. The corresponding spatial distribution is shown on the left-hand side of the figure. The amino acid is shown in stick representation. The oxygen atom of DMSO is depicted as an orange surface, and the methyl group is depicted as a gray mesh. The plots are calculated using the full 10-ns MD trajectory that starts with the lowest-energy NMR-derived three-dimensional structure of peptide sMTM7 embedded in DMSO (simulation no. 1).

the aromatic ring at a distance of 0.38 nm from the center of the aromatic ring (data not shown).

Solvation of the Side Chains of L734 and L736 of sMTM7 by DMSO. Analysis of the solvation shells of DMSO around the side chains of L734 and L736 in the S732-L736 segment of peptide sMTM7 gave identical results. The radial distribution function $g_{Me-Me}(r)$ shows that a shell of DMSO methyl groups is observed at a distance of 0.4 nm from the methyl groups of leucine (Figure 7 and Table 2). A second shell of DMSO molecules is observed in the $g_{Me-Me}(r)$ radial distribution function at 0.6 nm. However, the value of $g_{Me-Me}(r)$ at 0.6 nm is low and indicates that the DMSO molecules in this second solvent shell are almost like in the bulk phase.

Combining the results from the radial and spatial distribution functions, one can observe that DMSO molecules adequately solvate the side chains of leucine by pointing their methyl groups toward the methyl groups of leucine. As a result, a hydrophobic pocket surrounds the side chain of leucine (Figure 7).

The $g_{Me-Me}(r)$ shell at 0.4 nm is due to van der Waals interactions. The total van der Waals radius of each methyl group of leucine is approximately 0.29 nm as the van der Waals radii of hydrogen is 0.12 nm and of carbon is 0.17 nm. van der Waals contact between a methyl of leucine and a methyl of DMSO causes the addition of 0.1 nm to the internuclear distance between both methyls, as the methyls of DMSO are treated as a pseudogroup. The radial distribution function $g_{Me-O}(r)$ has a low intensity maximum at 0.7 nm, and this indicates that the oxygen atoms of the DMSO molecules in the first solvation shell are already almost randomly distributed.

Solvation of R735 of sMTM7 by DMSO. During the MD simulations the guanidine group of the arginine side chain is present as the protonated guanidinium form. Thus both constituting NH_2 groups indicated by nitrogen atoms $N_{\eta 1}$ and $N_{\eta 2}$ in Table 2 are identical. These NH_2 groups and the side chain NH group of R735 (nitrogen atom N_ε in Table 2) can all potentially form hydrogen bonds with the oxygen atom of DMSO. As a result, the MD calculations show a "helmet-like" coverage of the guanidinium group by oxygen atoms of DMSO (Figure 8). The N_η and the N_ε atoms have a layer of ordered oxygen atoms of DMSO molecules surrounding them with a maximum intensity in the radial distribution function at 0.3 nm (Figure 8). Again, this distance is consistent with the typical separation of donors and acceptors in a hydrogen bond between amide−

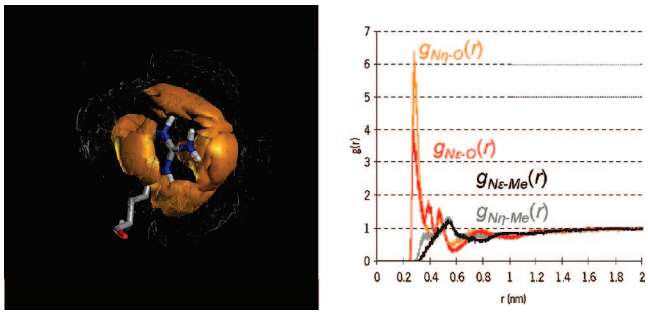

Figure 8. Radial distribution function (right) of the oxygen and methyl groups of DMSO around the $N_{\eta 1}H_2$, $N_{\eta 2}H_2$, and $N_\varepsilon H$ groups of R735. The corresponding spatial distribution function is shown on the left-hand side of the figure. The amino acid is shown in stick representation. The oxygen atom of DMSO is depicted as an orange surface, and the methyl group is depicted as a gray mesh. The plots are calculated using the full 10-ns MD trajectory that starts with the lowest-energy NMR-derived three-dimensional structure of peptide sMTM7 embedded in DMSO (simulation no. 1).

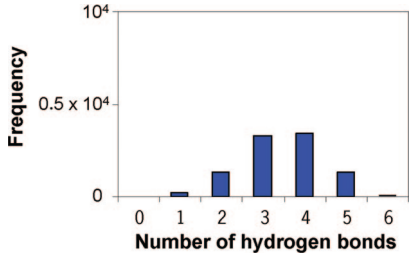

Figure 9. Histogram of the frequency of hydrogen bonds formed between the side chain of R735 and the oxygen atom of DMSO during the full 10-ns MD trajectory that starts with the lowest-energy NMR-derived three-dimensional structure of peptide sMTM7 embedded in DMSO (simulation no. 1).

hydroxyl (NH···OH) or amide−carbonyl (NH···O=C) groups.[33] The number of hydrogen bonds that is formed between the side chain of R735 and DMSO molecules is depicted in Figure 9. The maximum number of hydrogen bonds is six, however, on average three to four hydrogen bonds are found. Based on the distances found and on the number of hydrogen bonds, it is concluded that hydrogen bonding is the origin of the formation of the first DMSO solvation shell that surrounds the guanidine group of arginine.

Looking in more detail at the spatial distribution function, a more refined picture of the solvation of the guanidine group is obtained. In thecase of the $N_{\eta 1}$ and $N_{\eta 2}$ nitrogen atoms, the first $g_{N_\eta}-O(r)$ shell forms a band-like cloud coplanar to the plane formed by the three guanidinium nitrogens (Figure 8 and Supporting Information Figure 3). Peripheral to this $g_{N_\eta}-O(r)$ shell, a $g_{N_\eta}-Me(r)$ shell is found that has a maximum intensity in the radial distribution function at 0.39 nm (Figure 8 and Table 2). This distribution indicates that the DMSO molecules are oriented with their oxygen atoms pointing toward the nitrogen atoms of the guanidinium group and that the methyl groups of DMSO point toward the bulk solvent (as schematically illustrated in Figure 5). In the case of the N_ε nitrogen atom of R735, also a first $g_{N_\varepsilon}-O(r)$ solvation shell at 0.3 nm is observed. In addition, a second $g_{N_\varepsilon}-O(r)$ solvation shell is observed at 0.4 nm. This shell completes the helmet-like cloud seen in the spatial distribution function plot by covering the guanidinium group above and below the plane formed by the three guanidinium nitrogen atoms (Figure 8 and Supporting Information Figure 3). The location of this shell at 0.4 nm from N_ε indicates another type of interaction than formation of hydrogen bonds. In fact, this shell exists due to the positive charge of the guanidinium group that has a favorable interaction with the oxygen atom of DMSO (Figure 5). The $g_{N_\eta}-O(r)$ and $g_{N_\varepsilon}-O(r)$ shells at 0.5 nm arise due to presence of an organized first shell of DMSO molecules around the guanidinium group. The relatively low value of the radial distribution function of the second DMSO shell at 0.5 nm shows that this second shell is not ordered much.

Conclusions

In this work, MD simulations are used to study the solvation of a helical transmembrane peptide in DMSO. The 10-ns MD simulation shows that DMSO solvates the 25-residue peptide sMTM7 and that the backbone hydrogen bonds NH···O=C are not broken. Moreover, residues S732-L736 of the second helical region of peptide sMTM7 maintained their amino acid side chains fully embedded in the solvent, and no interactions between these side chains and between the backbone and these side chains are observed. DMSO solvates apolar, polar, and positively charged amino acid residues in a characteristic manner. Polar and positively charged amino acid side chains have dipole−dipole interactions with the oxygen atom of DMSO and form hydrogen bonds. Apolar residues become solvated by DMSO through the formation of a hydrophobic pocket in which the methyl groups of DMSO are pointing toward the hydrophobic side chain of the residue involved.

The comparison of the inner DMSO solvation shell around the side chains of charged and polar residues ($g_{X-O}(r)$ shells) with the one surrounding the side chain of leucine ($g_{Me-Me}(r)$ shell) shows that the shell around an apolar residue is less ordered and has a larger radius than the one surrounding charged and polar residues (Figures 6–8). This observation is the result of interactions between an apolar amino acid side chain and a hydrophobic pocket of DMSO being weaker than dipole−dipole interactions and hydrogen bonds between DMSO and a polar amino acid side chain. DMSO clearly has dual solvation properties as it exhibits polar as well as apolar features. These characteristic properties of DMSO enable it to mimic the natural environments of transmembrane peptides as these environments can be both of hydrophobic and hydrophilic nature. The results presented here support the growing evidence that DMSO can be used as a good membrane-mimicking solvent for transmembrane peptides that do not unfold due to the presence of DMSO.

Acknowledgment. This work was supported by Contract No. QLG-CT-2000-01801 of the European Commission (MIVase—New Therapeutic Approaches to Osteoporosis: targeting the osteoclast V-ATPase).

Supporting Information Available: (1) Detailed special distribution functions. (2) For each of the four amino acid residues studied, we produced a movie to allow a better understanding of the solvation of the residue side chain involved by DMSO. This material is available free of charge via the Internet at http://pubs.acs.org.

References and Notes

(1) Buck, M. *Q. Rev. Biophys.* **1998**, *31*, 297.
(2) *CRC Handbook of Chemistry and Physics*, 76th ed.; Lide, D. R., Ed.; CRC Press: Boca Raton, FL, 1995.
(3) Roccatano, D.; Colombo, G.; Fioroni, M.; Mark, A. E. *Proc. Natl. Acad. Sci. U.S.A.* **2002**, *99*, 12179.
(4) Yeagle, P. L.; Choi, G.; Albert, A. D. *Biochemistry* **2001**, *40*, 11932.
(5) Yeagle, P. L.; Danis, C.; Choi, G.; Alderfer, J. L.; Albert, A. D. *Mol. Vis.* **2000**, *6*, 125.
(6) Motta, A.; Temussi, P. A.; Wunsch, E.; Bovermann, G. *Biochemistry* **1991**, *30*, 2364.

(7) Duarte, A. M. S.; Wolfs, C. J. A. M.; Van Nuland, N. A. J.; Harrison, M. A.; Findlay, J. B. C.; Van Mierlo, C. P. M.; Hemminga, M. A. *Biochim. Biophys. Acta* **2007**, *1768*, 218.

(8) Duarte, A. M. S.; De Jong, E. R.; Wechselberger, R.; Van Mierlo, C. P. M.; Hemminga, M. A. *Biochim. Biophys. Acta* **2007**, *1768*, 2263.

(9) Bellanda, M.; Peggion, E.; Burgi, R.; van Gunsteren, W.; Mammi, S. *J. Pept. Res.* **2001**, *57*, 97.

(10) Jackson, M.; Mantsch, H. H. *Biochim. Biophys. Acta* **1991**, *1078*, 231.

(11) Zheng, Y. J.; Ornstein, R. L. *J. Am. Chem. Soc.* **1996**, *118*, 4175.

(12) Bürgi, R.; Daura, X.; Mark, A.; Van Gunsteren, W.; Bellanda, M.; Mammi, S.; Peggion, E. *J. Pept. Res.* **2001**, *57*, 107.

(13) Mierke, D. F.; Kessler, H. *J. Am. Chem. Soc.* **1991**, *113*, 9466.

(14) Van der Spoel, D.; Berendsen, H. J. C. *Biophys. J.* **1997**, *72*, 2032.

(15) Tzakos, A. G.; Fuchs, P.; Van Nuland, N. A. J.; Troganis, A.; Tselios, T.; Deraos, S.; Matsoukas, J.; Gerothanassis, I. P.; Bonvin, A. M. J. J. *Eur. J. Biochem.* **2004**, *271*, 3399.

(16) Kawasaki-Nishi, S.; Nish, T.; Forgac, M. *Proc. Natl. Acad. Sci. U.S.A.* **2001**, *98*, 12397.

(17) Kawasaki-Nishi, S.; Forgac, M. *FEBS Lett.* **2003**, *555*, 76.

(18) Vos, W. L.; Vermeer, L. S.; Hemminga, M. A. *Biophys. J.* **2007**, *92*, 138.

(19) Hesselink, R. W.; Koehorst, R. B. M.; Nazarov, P. V.; Hemminga, M. A. *Biochim. Biophys. Acta* **2005**, *1716*, 137.

(20) Vos, W. L.; Vermeer, L. S.; Wolfs, C. J. A. M.; Spruijt, R. B.; Hemminga, M. A. *Anal. Chem.* **2006**, *78*, 5296.

(21) DeLano, W. L. *The PyMOL Molecular Graphics System*; DeLano Scientific: Palo Alto, CA, 2002.

(22) Berendsen, H. J. C.; Van der Spoel, D.; Van Drunen, R. *Comput. Phys. Commun.* **1995**, *91*, 43.

(23) Van Der Spoel, D.; Lindahl, E.; Hess, B.; Groenhof, G.; Mark, A. E.; Berendsen, H. J. C. *J. Comput. Chem.* **2005**, *26*, 1701.

(24) Daura, X.; Mark, A. E.; Van Gunsteren, W. F. *J. Comput. Chem.* **1998**, *19*, 535.

(25) Liu, H.; Mueller-Plathe, F.; van Gunsteren, W. F. *J. Am. Chem. Soc.* **1995**, *117*, 4363.

(26) Berendsen, H. J. C.; Postma, J. P. M.; Van Gunsteren, W. F.; DiNola, A.; Haak, J. R. *J. Chem. Phys.* **1984**, *81*, 3684.

(27) Hess, B.; Bekker, H.; Berendsen, H. J. C.; Fraaije, J. G. E. M. *J. Comput. Chem.* **1997**, *18*, 1463.

(28) Kabsch, W.; Sander, C. *Biopolymers* **1983**, *22*, 2577.

(29) Fioroni, M.; Diaz, M. D.; Burger, K.; Berger, S. *J. Am. Chem. Soc.* **2002**, *124*, 7737.

(30) Van der Spoel, D.; Lindahl, E.; Hess, B.; Van Buuren, A. R.; Apol, E.; Meulenhoff, P. J.; Tieleman, D. P.; Sijbers, A. L. T. M.; Feenstra, K. A.; Van Drunen, R.; Berendsen, H. J. C. *Gromacs User Manual*, version 3.3, 2005.

(31) Yokogawa, D.; Sato, H.; Sakaki, S. *J. Chem. Phys.* **2006**, *125*, 114102.

(32) Johansson, A. C. V.; Lindahl, E. *Biophys. J.* **2006**, *91*, 4450.

(33) Baker, E. N.; Hubbard, R. E. *Prog. Biophys. Mol. Biol.* **1984**, *44*, 97.

(34) Nishi, T.; Forgac, M. *Nat. Rev. Mol. Cell. Biol.* **2002**, *3*, 94.

(35) Koradi, R.; Billeter, M.; Wüthrich, K. *J. Mol. Graphics* **1996**, *14*, 51.

JP076678J